JAAS

Accepted Manuscript

This is an *Accepted Manuscript*, which has been through the Royal Society of Chemistry peer review process and has been accepted for publication.

Accepted Manuscripts are published online shortly after acceptance, before technical editing, formatting and proof reading. Using this free service, authors can make their results available to the community, in citable form, before we publish the edited article. We will replace this *Accepted Manuscript* with the edited and formatted *Advance Article* as soon as it is available.

You can find more information about *Accepted Manuscripts* in the Information for Authors.

Please note that technical editing may introduce minor changes to the text and/or graphics, which may alter content. The journal's standard Terms & Conditions and the Ethical guidelines still apply. In no event shall the Royal Society of Chemistry be held responsible for any errors or omissions in this *Accepted Manuscript* or any consequences arising from the use of any information it contains.

ROYAL SOCIETY OF CHEMISTRY

www.rsc.org/jaas

Simultaneous determination of trace elements and lead isotope in silicate rock powders in fused glasses targets combined by boron nitride vessel and fsLA-(MC)-ICP-MS

Bao Zhian, Yuan Honglin*, Zong Chunlei, Liu Ye, Chen Kaiyun, Zhang Yulin

State Key Laboratory of Continental Dynamics, Department of Geology, Northwest University, Xi'an 710069, China

Abstract: A new glass-making method was developed to allow the in situ analysis of trace elements and lead isotopes in rock samples. The apparatus used to prepare homogeneous glass samples from silicate rock powder consisted of a small (450 mm^3) boron nitride vessel and a high-temperature furnace. The concentrations of trace elements have been measured by laser ablation inductively coupled plasma mass spectrometry (LA-ICP-MS) and lead isotopic compositions by femtosecond laser ablation multicollector inductively coupled plasma mass spectrometry (fsLA-MC-ICP-MS). The method was evaluated by analyzing glass disks fused from six geochemical reference materials (spanning the compositional range basalt - andesite - rhyolite). The measured 34 trace element contents match the reference values to within 15%, and the mean Pb isotopic ratios measured by fsLA-MC-ICP-MS agree with those obtained by solution nebulizer MC-ICP-MS

*Corresponding author: Yuan Honglin, email:yhlsklcd@126.com

within 2*s* uncertainty intervals. Using seven Faraday cups operating in static mode we were able to obtain $^{207}Pb/^{206}Pb$ and $^{208}Pb/^{206}Pb$ results with a factor of 2 - 3 improved precisions to previous single-collector sector-field ICPMS and LA-MC-ICP-MS. The accuracies of $^{207}Pb/^{206}Pb$ and $^{208}Pb/^{206}Pb$ values obtained by fsLA-MC-ICP-MS lie between −0.073% and +0.023%, which is well determined for geological research. Measured $^{208}Pb/^{204}Pb$, $^{207}Pb/^{204}Pb$ and $^{206}Pb/^{204}Pb$ isotope ratios for the USGS reference RGM-2 (20 μg g^{-1} total Pb) and BCR-2 (11 μg g^{-1} total Pb) agree within 0.029% and 0.055% respectively of the preferred values. For GSR-3 (4.27 μg g^{-1} total Pb), the accuracies of the $^{208}Pb/^{204}Pb$, $^{207}Pb/^{204}Pb$ and $^{206}Pb/^{204}Pb$ ratio obtained by fsLA-MC-ICP-MS lie between −0.064% and -0.004% with the accepted external precision of <0.15% (1RSD), which are improved over previous LA-MC-ICP-MS data in terms of quantification limits. We also provide precise Pb isotopic data for the reference materials GSR-2, GSR-3, QLO-1, and RGM-2 obtained by solution nebulizer MC-ICP-MS. Our method is simpler, cheaper and faster to determinate trace element and Pb isotopic ratios in geological samples, while retaining similar levels of accuracy and precision.

Keywords: Pb isotope, Trace elements, fsLA-MC-ICP-MS, hermetic boron nitride crucible, reference materials, precision, accuracy.

Introduction

Laser ablation-(multi-collector) inductively coupled plasma mass spectrometry (LA-(MC)-ICP-MS) is a powerful tool for in situ determination of major and trace

elements concentrations and isotopic ratios of geological, environmental, forensic, archaeological and other solid samples.[1-18] LA-(MC)-ICP-MS analysis of solids provides several advantages over solution ICP-MS, including minimal sample preparation, low blanks, high spatial resolution (10-100 μm) and rapid analysis times (generally <3 min per analysis), which make LA-(MC)-ICP-MS a cost-effective and attractive analytical tool not only for microanalysis of very small heterogeneous samples[19], but also for bulk analysis of homogeneous samples, such as fused glass disks[5, 9, 20, 21] and pressed powder pellets.[22, 23] With the development of LA-(MC)-ICP-MS, geological, environmental, forensic, archaeological and industrial applications have been enhanced through integrating micro and bulk geochemical determinations of major and trace elements concentrations and isotopic compositions.

Fused glass disks are generally more homogenous than pressed powder pellets and are therefore preferable for laser ablation analysis. Fusing techniques using an iridium strip heater (1300 - 1800 °C) with or without flux have been developed for the LA-ICP-MS analysis of silicate rock samples.[5, 9, 20, 21] Recently, Zhu *et al.*[9] used a hermetic boron nitride (BN) crucible combined with a molybdenum-strip heater to prepare fused glasses from silicate rocks for LA-ICP-MS analysis.

In this work, fused glasses were prepared without a flux in a hermetic BN crucible and a single high-temperature furnace. Their trace element contents and Pb isotopic compositions were then measured by fsLA-(MC)-ICP-MS. The applicability of this approach is evaluated for six rock powders of different compositions. We also present the first precise Pb isotopic data for the reference materials RGM-2, QLO-1,

GSR-2, and GSR-3, obtained by solution nebulizer (SN) MC-ICP-MS.

Experiments

Hermetic Boron Nitride Vessel and Furnace

A hermetic BN vessel was designed (Figure 1) to melt 500 mg rock powder at 1400 °C and was then quenched in liquid nitrogen. This crucible (450 mm^3) was placed in a high-temperature furnace and heated to a stable temperature 1400 °C (as measured via a thermocouple) using high-resistance silicon molybdenum bars (purity = 99.9%, melting point = 2000 °C) under argon gas flow (1.0 L min^{-1}) to maintain an inert atmosphere.

Sample preparation

Experiments were performed on four reference materials (BCR-2 (basalt powder), AGV-2 (andesite powder), OLO-1 (quartz latite powder), and RGM-2 (rhyolite powder)) obtained from United States Geological Survey (USGS) and two reference materials (GSR-3 (GBW07105, basalt powder) and GSR-2 (GBW07104, andesite powder)) (Chinese) obtained from National Research Center for Certified Reference Materials. All samples were prepared directly from 200-mesh powders dried at 105 °C in an oven for 1 h prior to melting. The BN crucibles (cleaned ultrasonically for 10 min in 2% v/v HNO_3) were heated at 500°C for 2 min to remove all volatile components before use. The high-temperature furnace achieved to 1400 °C from room temperature consuming about 40 minutes. The samples were weighed (500 mg),

poured into a crucible, and compacted tightly using a stainless steel rod. Each sealed crucible was then set into the high-temperature furnace setting at 1400 °C and quickly closed the high-temperature furnace. The furnace dropped to 1300 °C during the process and rose to 1400 °C consuming 1 min. The sealed crucible was then heated during 1 min to melt the rock powder. Note that temperatures lower than this may leave some unmelted powder in the glass, while lead may evaporate at higher temperatures.[24, 25] The BN crucible was removed from the furnace using tongs and rapidly immersed in liquid nitrogen to separate the fused glass from the crucible. Argon was insufflated into the furnace with 1.0 L min^{-1} flow in the whole process. The resultant glasses were mounted in resin, labeled, and then polished to obtain an even surface. The glasses were observed under a microscope to reveal any precipitates or crystallization, and then cleaned for 1 min in an ultrasonic bath containing 2% v/v HNO_3 prior to LA-ICP-MS and fsLA-MC-ICP-MS analyses.

Instruments and operating conditions

The trace element contents in the different glasses were measured at the State Key Laboratory of Continental Dynamics, Northwest University, Xi'an, using an Agilent 7500 ICP-MS instrument attached to a 193 nm excimer laser ablation system (Geolas 2005). All the measurements were performed in time-resolved mode with helium as the carrier gas. The carrier flow was optimized to obtain maximum signal intensity for $^{238}U^+$, while keeping the ThO^+/Th^+ ratio below 0.5% and the U^+/Th^+ ratio close to 1 for the reference glass (SRM 610, National Institute of Standards and Technology).

Each individual run consisted of a background acquisition for approximately 20 s (gas blank) followed by 50 s for each analyzed region of the sample. The operational parameters for the 193 nm and femtosecond laser ablation systems and 7500 ICP-MS instrument are listed in Table 1.

The Pb isotopic compositions of the fused glasses were measured using a Nu II MC-ICP-MS instrument (Nu Instruments, Wrexham, UK) attached to an NWR UP Femto femtosecond laser ablation system (ESI, USA) with a Quantronix Integra-HE Ti: sapphire femtosecond laser amplifier. This system is regenerative and offers multipass ablation based on the chirped pulse amplification technique. The laser outputs an ultraviolet (266 nm wavelength) Gaussian beam with third-harmonic generation. The pulse duration was less than 130 fs; the output energy was greater than 500 μJ (at 250 Hz) in the ultraviolet region (k = 266 nm); and the sample surface fluence was greater than 7 J cm^{-2}; repetition frequencies of 1-50 Hz, 125 Hz, and 250 Hz were used along with 13 adjustable apertures (laser ablation spot size of 1-65 μm). The instrument was equipped with a color charge-coupled device camera and a two-volume chamber.

The Nu Plasma multi-collector ICP-MS represents the latest generation of double-focussing mass spectrometers. The new collector has sixteen Faraday detectors for greater flexibility, and its five full-size discrete dynode multipliers enable the determination of precise isotope ratios, even for isotopes with very low abundance. Its zoom optics system allows the observation of instant changes in dispersion and perfect peak overlap without slow and potentially unreliable detector

movement. An Aridus II TM (CETAC, USA; 100 μL min^{-1} PFA nebulizer) desolvation system was used, which enhances the MC-ICP-MS sensitivity by more than a factor of 10 for oxide ratios below 0.03% (CeO^+/Ce^+). The operational parameters Nu MC-ICP-MS instrument are also listed in Table 1.

Analysis and data reduction for trace element

Due to the major element composition is very different from any geological matrix, which may lead to significant analytical biases due to matrix effects.[1, 2, 26] Therefore, reference glasses with natural compositions were used for calibration. Because the abundances of some trace elements in reference glasses with natural compositions are too low to permit a precise calibration, we used three USGS reference glasses (BCR-2G, BHVO-2G and BIR-1G from USGS)[27] to ensure that the concentrations of all trace elements were high enough to provide a precise primary calibration. Off-line selection and integration of background and ablation signals, and time-drift correction and quantitative calibration were performed by ICPMSDataCal.[1] All count rates for each analysis were firstly normalized to the ^{29}Si count rate, and then a time-drift correction was applied by using a linear interpolation (with time) for every ten analyses using the variations of signal intensity ratios of NIST SRM 610 (NIST SRM 610 + eight sample analyses + NIST SRM 610).

Analysis strategy and data reduction for lead isotope

The line scan ablation mode has distinct advantages over the spot ablation in terms of

uniformity throughout the course of ablation, eliminating mass-dependent variation due to in situ fractionation of measured elemental isotopic ratios.[28] Pre-ablation with high scanning speed (100 μm s^{-1}) was carried out before sample analyses to remove any contamination or modification of sample surface after leaching. So, a high line scanning rate of 10 μm s^{-1} at full power was found to be appropriate to adequately ablate the samples mass and minimize the in situ fractionation effect. To ensure a representative measurement of the bulk sample, we used a wide beam diameter (65 μm) and a long line scanning length (500 μm), that is, an area of about 3×10^4 μm^2 was sampled. A depth of about 30 μm with the area would ablate 1×10^6 μm^3 of sample volume, which is approximately microgram of sample consumed due to the density of glass is assumed to be approximately 2.4 g cm^{-3}.[29] About 50 mg sample by twenty line scans are sufficient to represent the bulk composition.

The Tl aerosol from the desolvator and the sample aerosol from the femtosecond laser ablation cell were mixed homogeneously in a glass container and then introduced into the ICP chamber for atomization and ionization. Thallium was used to monitor and correct for instrumental mass discrimination. The uptake rate of the PFA nebulizer was 100 μL min^{-1}. Helium was used as the carrier gas for laser ablation. A detailed schematic diagram of the experimental setup can be found in reference.[10]

During the analysis, L4, L3, L2, L1, Ax, H1, and H2 Faraday cups were used to collect the ^{202}Hg, ^{203}Tl, ^{204}Hg+^{204}Pb, ^{205}Tl, ^{206}Pb, ^{207}Pb, and ^{208}Pb ion beams, respectively. The ^{202}Hg signal was measured to deduct the isobaric interference from ^{204}Hg on ^{204}Pb. The calculated and determined interference of ^{204}Hg on ^{204}Pb was

achieved using the natural abundance ratio $^{204}Hg/^{202}Hg = 0.229883$ ($^{202}Hg = 0.29863$ and $^{204}Hg = 0.06865$) adjusted for instrumental mass fractionation as monitored by the $^{205}Tl/^{203}Tl$ ratio. The Tl aerosol was continuously sampled to monitor and account for changes in the instrumental conditions between the injection of the sample and the wash step.

The Pb isotope ratios were measured by time-resolved MC-ICP-MS, with an integration time of 0.1 s, and laser ablation was performed in line scan mode at 10 μm s^{-1} with the laser beam focused on the sample surface. Each scan consisted of a background measurement for 20 s, followed by an additional 50 s of ablation for signal collection and 120 s of wash time to reduce memory effects. The laser spot size (65 μm) were chosen to collect enough Pb signal from the fused glasses.

The $^{204}Hg/^{202}Hg$ natural abundance ratio (0.229883) was used to calculate and determine the interference from ^{204}Hg on the ^{204}Pb intensity obtained. Similarly, the $^{205}Tl/^{203}Tl$ ratio (2.3889) and an exponential law were used to correct the instrumental mass discrimination between Hg and Pb. The National Institute of Standards and Technology (NIST) reference sample SRM 610 was analyzed for quality control once every six sampling points during the time-resolved analysis. The data reduction procedure is described in detail in references.[10-12]

Results and discussion

Trace element concentration homogeneity of the fused glasses

The six fused glasses were first observed under a microscope (Figure 2). Many small

bubbles are visible in the fused glasses of the RGM-2 and QLO-1 powders (Figure 2a, b), while for the AGV-2, GSR-2, and BCR-2 samples, the bubbles are larger (Figure 2c,-e). In contrast, the GSR-3 glass is free of bubbles (Figure 2f). These bubbles may stem from the high viscosity of the rhyolite melt, which could have been reduced by increasing the melting temperature. This was nonetheless maintained at 1400 °C to reduce the risk of Pb loss through evaporation.[24, 25]

Significant loss of the volatile elements (e.g., Cs, Ce, Pb, Zn) happened using the traditional single Ir-strip heater due to high melting temperatures (>1600 ℃) and long melting time.[5] Eight single-spot LA-ICP-MS analyses from one edge to another were performed on each fused glass to evaluate the element loss during melting in a closed crucible. The results (Figure 3 and Table 2) indicate that the RSD of Cs and Pb were better than 13%, mostly better than 10%. The average contents of Pb and Cs were consistent with the preferred values within the uncertainty, except for Cs in GSR-3 due to low concentration and Pb in QLO-1 (discussed in next section). These observations suggest that element volatilization during the high-temperature melting was effectively suppressed.

Eight single-spot LA-ICP-MS analyses were performed on each fused glass to evaluate the homogeneity of their trace element contents. Most trace element contents generally matched the preferred values to within 15% (Figure 3). Relatively high relative deviations in some elements (e.g. Tm, Ta, Tb, Lu) may have been caused by their low concentrations. The measured Zn in the fused glasses was higher than the preferred values by 4-26 %, which may have resulted from polyatomic ion

interferences (i.e., $^{48}Ti^{18}O$, $^{49}Ti^{17}O$, $^{50}Ti^{16}O$ and $^{50}Cr^{16}O$ on ^{66}Zn)[9]. Although the measured values of V, Cr, Co and Ni were generally within 15%, the RSDs were relatively high, which was caused by the use of BN as a vessel material. Wendlandt et al. (1982)[30] indicated that BN may reduce transition metal ions such as Ni^{2+} and Fe^{2+} to the metallic state due to its strong reducing power at high temperature. These high RSD values for some transition metal elements were also observed by Zhu et al. (2013)[9], which suggested that using BN vessel was limited for some transition metal elements. The relative deviations were better than 15%, except for Cr in RGM-2 and QLO-1 due to its low contents (4.02 μg g^{-1} in RGM-2, 3.20μg g^{-1} in QLO-1). The results showed that the V, Cr, Co and Ni were not homogenous and more samples were needed to be analyzed to obtain representative results, such as line scan technique or bigger laser spots (> 90 μm). The good accuracy and low relative standard deviations values in Zr, Hf, Th and U in QLO-1 imply that refractory mineral zircon was melted and did not recrystallize during the quenching process.

The RSDs of the lead concentrations obtained were lower than 6.8%, except for the GSR-3 glass (13.0%), because of its low lead content (about 4.27 μg g^{-1}, see Table 2). Compared to the reference concentrations, the relative errors for the values measured here are less than 5% (in absolute value, see Figure 3 and Table 2), except for QLO-1 (-32.3%). The low RSDs suggest that the proposed method produces fused glasses with homogeneous Pb concentrations. Figure 4 shows that the correlation between the measured and reference concentrations is almost perfect (R^2 = 0.9993), suggesting that the amount of lead lost by evaporation during the melting process is

negligible. Only for QLO-1 is the measured concentration lower than the reference value (taken from the GeoReM database). The lead contents published for QLO-1 range from 20 to 23.9 μg g^{-1}.[31] As measured here using high-temperature and high-pressure Teflon bomb digestion ICP-MS, the lead content of QLO-1 is 13.5 ± 0.1 ppm (n = 3), which is in perfect agreement with the value obtained for the fused glass (Table 2). Besides, the relative errors for Pb, Th and U in five USGS reference powders (BHVO-2, AGV-2, BCR-2, GSP-2 and QLO-1) are better than 6% at the same batch, except for Pb in QLO-1(see attachment data). The results show that some resistant minerals are absolutely dissolved using high-pressure Teflon bomb. The low Pb contents in QLO-1 may be caused by the heterogeneity or complication from loosely bound Pb (weathering and contamination during milling).

Compared with the data produced by iridium-strip heater[5], the method established in this study provides improved suppression of element volatilization (e.g., Sc, Cs and Pb). Relatively deviation within 15% for the remaining trace elements were achieved by the Zhu *et al.*[9] and Stoll *et al.*[5]

Pb homogeneity and accuracy in fused glasses

Prior to melting the six rock powders, we measured their bulk lead isotopic compositions by chemical digestion followed by chromatography. The NIST sample SRM 981 was analyzed 44 times over a period of six months to evaluate the accuracy of the Pb isotope measurements based on Tl calibration (Table 3). The values obtained agree with both published and compiled values within the corresponding 2*s*

uncertainties.[10, 32, 33] Similarly for BCR-2 (n = 14) and AGV-2 (n = 18), the measured isotopic ratios are within 2*s* of the expected values.[34-37] Table 3 also lists the Pb isotope ratios in GSR-3, GSR-2, RGM-2, and QLO-1 as measured by SN-MC-ICP-MS (n = 8), against which the values measured on fused glasses by fsLA-MC-ICP-MS are compared in the following section.

Twenty measurements were performed across the surface of each fused glass. The mean Pb isotope ratios, in-run precision (RSE), external precision (RSD) and standard deviation (SD) of six fused samples are shown in Table 4. The in-run precision on the $^{208}Pb/^{204}Pb$, $^{207}Pb/^{204}Pb$, and $^{206}Pb/^{204}Pb$ ratios obtained in RGM-2 are 0.041%, 0.041%, and 0.041%, increased to 0.191%, 0.191%, and 0.191% in GSR-3. The increased RSE in $^{206,207,208}Pb/^{204}Pb$ caused by the decreased Pb contents in fused glasses from 20 μg g^{-1} to 4.27 μg g^{-1}. The trend also can be observed from the RSE values of $^{207,208}Pb/^{206}Pb$ in fused glasses. An in-run precision of about 0.041% for $^{206,207,208}Pb/^{204}Pb$ and 0.005% for $^{207,208}Pb/^{206}Pb$ was reached for RGM-2. For a twenty-line analyses and a given laser ablation parameters of 10 μm s^{-1}, 250 Hz and 65 μm, the external precision (1RSD) on the $^{206,207,208}Pb/^{204}Pb$ ratios obtained in fused glasses increased from 0.026% in RGM-2 to 0.153% in GSR-3. The increased RSD in $^{206,207,208}Pb/^{204}Pb$ was actually caused by the increased standard deviation (1SD), which increased from 0.004 to 0.054. The higher standard deviation in GSR-3 for $^{206,207,208}Pb/^{204}Pb$ is easily interpreted by the lower ^{204}Pb signal, while Hg filter designed by Yuan[12] and $^{204}Hg/^{202}Hg$ natural abundance ratio (0.229883) were used to subtract the interference from ^{204}Hg on the ^{204}Pb intensity obtained. The similar RSD

in six fused glasses is about 0.03% - 0.07% for $^{207,208}Pb/^{206}Pb$, which is independence with the ^{204}Pb.

The mean Pb isotopic compositions measured for the six fused glasses also agree well with the reference values (relative error <0.064%), with Figures 5 and 6 highlighting the almost perfect linear correlations between the two datasets (R^2 = 0.9998, 0.9996, 0.99996, 0.9955, and 0.9999, for the $^{208}Pb/^{206}Pb$, $^{208}Pb/^{204}Pb$, $^{207}Pb/^{206}Pb$, $^{207}Pb/^{204}Pb$, and $^{206}Pb/^{204}Pb$ concentration ratios, respectively). $^{207,208}Pb/^{206}Pb$ values for NIST SRM 612 and NIST SRM 610 are within 2*s* uncertainty intervals compared to the published values by Jochum *et al.*,[17] Chen *et al.*[10] and Shaheen and Fryer.[38] Based on low RSE and RSD for $^{207,208}Pb/^{206}Pb$, the mean $^{207,208}Pb/^{206}Pb$ values of 6 independent LA-MC-ICP-MS analyses of six fused glasses are identical within 0.07% with the reference values. These relatively deviation are similar to external precision of the LA-MC-ICP-MS (0.03% - 0.07%) indicating that fused glasses are homogeneous and calibration errors are small.

For six fused glasses, accuracies and precisions of $^{207,208}Pb/^{206}Pb$ are often more accurate and precise than that of $^{206,207,208}Pb/^{204}Pb$, ascribed to the error associated with measurement of ^{204}Pb. The difference is most marked where the lead content of the glass is very low. For instance, although the mean twenty-line scans values for $^{206,207,208}Pb/^{204}Pb$ are within 0.064% compared with reference values, the single ratio fluctuates in GSR-3 fused glass from 37.748 to 37.914, and the external precision and in-run precision were higher (0.14% for 1RSD and 0.19% for 1RSE). Whereas lower the external precision and in-run precision (0.039% for 1RSD and 0.015% for 1RSE)

were obtained for $^{207,208}Pb/^{206}Pb$. Obviously, the Pb contents play the critical role in accuracies and precisions of $^{206,207,208}Pb/^{204}Pb$.

Comparison with other investigation

It is difficult to compare the results of our lead isotope measurements of six fused glasses to previous investigations due to differences in glasses prepared process, instruments, analysis protocol, laser ablation parameters, analyses number and lead intensity. Figure 7 provides a comparison between the external precision and accuracy both $^{208}Pb/^{204}Pb$ and $^{208}Pb/^{206}Pb$ determined in this study with previous LA-MC-ICP-MS and single-collector, LA-SF-ICPMS investigation. Using 7 Faraday cups operating in static mode we were able to obtain $^{207,208}Pb/^{206}Pb$ results with a factor of 2-3 improved precisions to previous single-collector sector-field ICPMS[14, 15, 17] and LA-MC-ICP-MS using multiple Faradays combined ion counters[18] and multiple ion counters[16]. The $^{207,208}Pb/^{206}Pb$ values obtained using different method, different laser ablation and mass spectrometry are within 0 - 0.1% agree with the high-precision TIMS and MC-ICP-MS data. The LA-SF-ICP-MS results for $^{206,207,208}Pb/^{204}Pb$ are less precision (0.7 - 2.1%) and accuracy (0.4 - 2.0%) for the low abundance of ^{204}Pb and correction from the ^{204}Hg interference. The precision of $^{206,207,208}Pb/^{204}Pb$ results in this study with a factor of 2 - 4 higher than that obtained by previous LA-MC-ICP-MS study based on about 10 μg g^{-1} contents in BCR-2G and T1-G. The accuracy is within 0.04% using LA-MC-ICP-MS, better than that obtained by LA-SF-ICPMS. The reason for the improved accuracy in $^{206,207,208}Pb/^{204}Pb$

compared to LA-SF-ICP-MS depends on the correction from ^{204}Hg interference and stable instrument condition without changing magnet. A reference material with low Pb contents (BCR-2G) must to analyzed to cross-calibrate detectors and be a bracketing reference materials to correct for instrument mass bias using MICs to measure lead or mercury. Our method avoid to analysis a lot of standard glasses compared with previous method using MICs, improving efficiency during laser ablation. The Table 4 and Figure 7 showed that the precision and accuracy of $^{206,207,208}Pb/^{204}Pb$ and $^{207,208}Pb/^{206}Pb$ in NIST610 and NIST612 obtained in this study agreed well with previously values.[10, 17, 38] The standard deviation and relative standard deviation of six fused glasses ploted in the fitted curve, which showed good correlations between the standard deviation and relative standard deviation of $^{208}Pb/^{204}Pb$ ratios with Pb concentration by Chen *et al.,*[10]. So, the method(1400℃ & 1min) in this study was chose to obtain fused glasses, which were used to determine the lead isotope compared with that obtained by bulk solution MC-ICP-MS.

Conclusion

A hermetic BN crucible (450 mm^3) and a high-temperature furnace have been used to directly prepare fused glasses from rock powders (500 mg). This setup offers a cost-effective and efficient means to prepare samples of any silicate rocks for trace elements and Pb isotope measurements by LA-ICP-MS and fsLA-MC-ICP-MS. Pb is evenly distributed in the fused glasses and the rapid and hermetic melting process ensures that Pb volatilization is negligible. Analyses of geochemical reference

materials (spanning the compositional range basalt - andesite - rhyolite) indicated that the measured trace element contents generally matched the preferred values within 15%. In situ lead isotope measurements using an array of Faraday cups produces results with similar or improved precisions and accuracies compared to mixed Faraday-ion counter multi-collector and single-collector, sector-field measurements of lead isotope ratios in silicate glasses from 4 to 20 μg g^{-1}. The Pb isotope ratios measured by fsLA-MC-ICP-MS for different geochemical reference materials (basalt, andesite, and rhyolite) prepared in this way are in good agreement with (viz. within 2*s* of) published data, or in the absence thereof, with values obtained using SN-MC-ICP-MS. Furthermore, precise Pb isotopic data are reported for the first time for reference materials RGM-2, GSR-2, GSR-3, and QLO-1 using traditional dissolution MC-ICP-MS.

Acknowledgements

We would like to thank the editor and anonymous reviewers who helped to improve this manuscript. This work was co-supported by the National Natural Science Foundation of China (Grant Nos. 41427804, 41421002, 41373004), the Program for Changjiang Scholars and Innovative Research Team in University (Grant No. IRT1281), and the MOST Research Foundation from the State Key Laboratory of Continental Dynamics (Grant No. BJ08132-1, 207010021).

References

1. Y. Liu, Z. Hu, S. Gao, D. Günther, J. Xu, C. Gao and H. Chen, *Chemical Geology*, 2008, 257, 34-43.
2. K. P. Jochum, B. Stoll, K. Herwig and M. Willbold, *Journal of Analytical Atomic Spectrometry*, 2007, 22, 112-121.
3. K. E. Jarvis and J. G. Williams, *Chemical Geology*, 1993, 106, 251-262.
4. K. P. Jochum, M. Willbold, I. Raczek, B. Stoll and K. Herwig, *Geostandards and Geoanalytical Research*, 2005, 29, 285-302.
5. B. Stoll, K. P. Jochum, K. Herwig, M. Amini, M. Flanz, B. Kreuzburg, D. Kuzmin, M. Willbold and J. Enzweiler, *Geostandards and Geoanalytical Research*, 2008, 32, 5-26.
6. D. Gunther and C. A. Heinrich, *Journal of Analytical Atomic Spectrometry*, 1999, 14, 1369-1374.
7. R. L. Green and R. J. Watling, *Journal of Forensic Sciences*, 2007, 52, 851-859.
8. B. Gratuze, *Journal of Archaeological Science*, 1999, 26, 869-881.
9. L. Zhu, Y. Liu, Z. Hu, Q. Hu, X. Tong, K. Zong, H. Chen and S. Gao, *Geostandards and Geoanalytical Research*, 2013, 37, 207-229.
10. C. Kaiyun, Y. Honglin, B. Zhian, Z. Chunlei and D. Mengning, *Geostandards and Geoanalytical Research*, 2014, 38, 5-21.
11. H. Yuan, K. Chen, B. ZhiAn, C. Zong, M. Dai, C. Fan and C. Yin, *Chinese Science Bulletin*, 2013, 58, 3914-3921.
12. H. Yuan, C. Yin, X. Liu, K. Chen, Z. Bao, C. Zong, M. Dai, S. Lai, R. Wang and S. Jiang, *Science China Earth Sciences*, 2015, 1713-1721.
13. A. Simonetti, M. R. Buzon and R. A. Creaser, *Archaeometry*, 2008, 50, 371-385.
14. K. P. Jochum, J. Pfänder, J. D. Woodhead, M. Willbold, B. Stoll, K. Herwig, M. Amini, W. Abouchami and A. W. Hofmann, *Geochemistry, Geophysics, Geosystems*, 2005, 6, n/a-n/a.
15. K. P. Jochum, B. Stoll, K. Herwig and M. Willbold, *Journal of Analytical Atomic Spectrometry*, 2006, 21, 666-675.
16. A. Kate Souders and P. J. Sylvester, *Journal of Analytical Atomic Spectrometry*, 2008, 23, 535-543.
17. K. P. Jochum, B. Stoll, K. Herwig, M. Amini, W. Abouchami and A. W. Hofmann, *International Journal of Mass Spectrometry*, 2005, 242, 281-289.
18. B. Paul, J. D. Woodhead and J. Hergt, *Journal of Analytical Atomic Spectrometry*, 2005, 20, 1350-1357.
19. A. MüLLER, M. WIEDENBECK, A. M. V. D. KERKHOF, A. KRONZ and K. SIMON, *European Journal of Mineralogy*, 2003, 15, 747-763.
20. S. M. Eggins, *Geostandards Newsletter*, 2003, 27, 147-162.
21. Z. Yu, M. D. Norman and P. Robinson, *Geostandards Newsletter*, 2003, 27, 67-89.
22. D. Garbe-Schonberg and S. Muller, *Journal of Analytical Atomic Spectrometry*, 2014, 29, 990-1000.
23. M. Tibi and K. G. Heumann, *Journal of Analytical Atomic Spectrometry*, 2003, 18, 1076-1081.
24. Z. Bao, G. He, K. Chen, J. Song, H. Yuan and X. Liu, *Geochimica*, 2011, 40, 223-236. (In Chinese with English abstract)
25. Z. Bao, H. Yuan, K. Chen, J. Song, M. Dai and C. Zong, *ROCK AND MINERAL ANALYSIS*, 2011, 30, 521-527. (In Chinese with English abstract)
26. Z. Hu, Y. Liu, L. Chen, L. Zhou, M. Li, K. Zong, L. Zhu and S. Gao, *Journal of Analytical Atomic*

Spectrometry, 2011, 26, 425-430.

27. USGS, 2002, http://minerals.cr.usgs.gov/geo_chen_stand/.
28. I. Kroslakova and D. Gunther, *Journal of Analytical Atomic Spectrometry*, 2007, 22, 51-62.
29. A. J. Walder, I. D. Abell, I. Platzner and P. A. Freedman, *Spectrochimica Acta Part B: Atomic Spectroscopy*, 1993, 48, 397-402.
30. R. F. Wendlandt, J. S. Huebner and W. J. Harrison, *American Mineralogist*, 1982, 67, 170-174.
31. K. P. Jochum, U. Nohl, K. Herwig, E. Lammel, B. Stoll and A. W. Hofmann, *Geostandards and Geoanalytical Research*, 2005, 29, 333-338.
32. S. J. G. Galer and W. Abouchami, *Mineralogical Magazine*, 1998, 62A, 491-492.
33. M. F. Thirlwall, *Chemical Geology*, 2000, 163, 299-322.
34. J. Baker, D. Peate, T. Waight and C. Meyzen, *Chemical Geology*, 2004, 211, 275-303.
35. D. Weis, B. Kieffer, C. Maerschalk, J. Barling, J. de Jong, G. A. Williams, D. Hanano, W. Pretorius, N. Mattielli, J. S. Scoates, A. Goolaerts, R. M. Friedman and J. B. Mahoney, *Geochemistry, Geophysics, Geosystems*, 2006, 7, Q08006.
36. K. D. Collerson, B. S. Kamber and R. Schoenberg, *Chemical Geology*, 2002, 188, 65-83.
37. M. Elburg, P. Vroon, B. van der Wagt and A. Tchalikian, *Chemical Geology*, 2005, 223, 196-207.
38. M. Shaheen and B. J. Fryer, *Journal of Analytical Atomic Spectrometry*, 2010, 25, 1006-1013.

Figure captions

Figure 1. Schematic diagram of the hermetic BN crucible and the high-temperature furnace.

Figure 2. Optical micrographs of fused glasses prepared from the powders of (a) RGM-2, (b) QLO-1, (c) AGV-2, (d) GSR-2, (e) BCR-2, and (f) GSR-3 reference materials. The $^{206,207,208}Pb/^{204}Pb$ ratios in RGM-2 fused glasses indicated that the lead isotope compositions varied erratically from one brim to another. The black dotted line show the average value obtained by SN-MC-ICP-MS and the gray region show the 2*s* uncertainty range. The error bars represent ±1*s*.

Figure 3. accuracy and precision of analyzing RGM-2, QLO-1, AGV-2, GSR-2, BCR-2 and GSR-3 fused glasses using LA-ICP-MS.

Figure 4. Pb concentrations measured in fused glasses of reference materials GSR-3, GSR-2, BCR-2, AGV-2, QLO-1, and RGM-2, plotted against the corresponding reference values. The dashed lines show the uncertainty range (±10%). The two datasets are highly correlated ($R^2 = 0.9993$) and all points are within their associated 1*s* ranges.

Figure 5. Measured vs. reference $^{208}Pb/^{204}Pb$, $^{207}Pb/^{204}Pb$, and $^{206}Pb/^{204}Pb$ isotope ratios in fused glasses prepared from six reference materials. The error bars represent ±1*s*. The values obtained by fsLA-MC-ICP-MS are within ±0.064% of the reference ratios.

Figure 6. Measured vs. reference $^{208}Pb/^{206}Pb$ and $^{207}Pb/^{206}Pb$ isotope ratios in fused glasses prepared from six reference materials. The error bars represent ±1*s*. The

values obtained by fsLA-MC-ICP-MS are within 1*s* of the reference ratios with clear linear correlations between the datasets (R^2 = 0.9998 for $^{208}Pb/^{206}Pb$ and R^2 = 0.99996 for $^{207}Pb/^{206}Pb$).

Figure 7. Comparison of the external precision and relative error of $^{208}Pb/^{206}Pb$ and $^{208}Pb/^{204}Pb$ as a function of line scan in this study and other LA-MC-ICP-MS and single-collector LA-SF-ICM-PS investigations. The accuracy and precision of GSR-3 and BCR-2, which have similar Pb contents with T1-G and ATHO-G, are used to compare with previous values in this work.

Table captions:

Table 1. Operational parameters for ICP-MS and MC-ICP-MS instruments and 193 nm and femtosecond laser ablation systems.

Table 2. Results for the fused RGM-2, QLO-1, AGV-2, GSR-2, BCR-2 and GSR-3 glasses by LA-ICP-MS.

Table 3. Pb isotope ratios for seven reference materials, as measured by SN-MC-ICP-MS.

Table 4. Pb isotope ratios measured in fused glasses of six reference materials, NIST SRM 610 and NIST SRM 612 by fsLA-MC-ICP-MS and confirmed by SN-MC-ICP-MC.

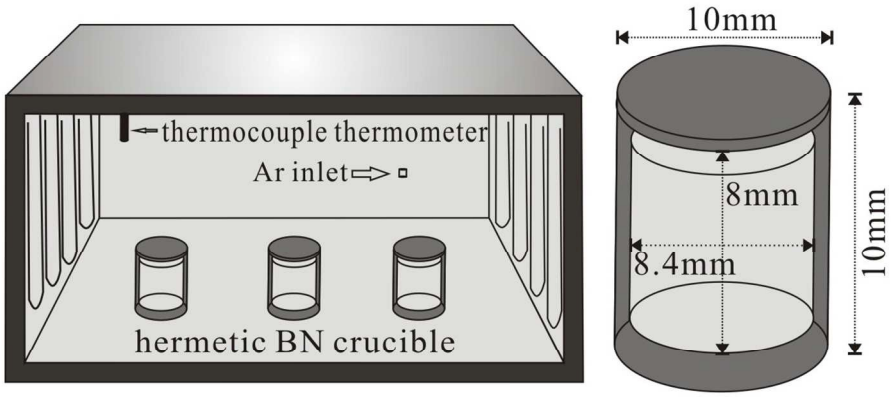

123x60mm (300 x 300 DPI)

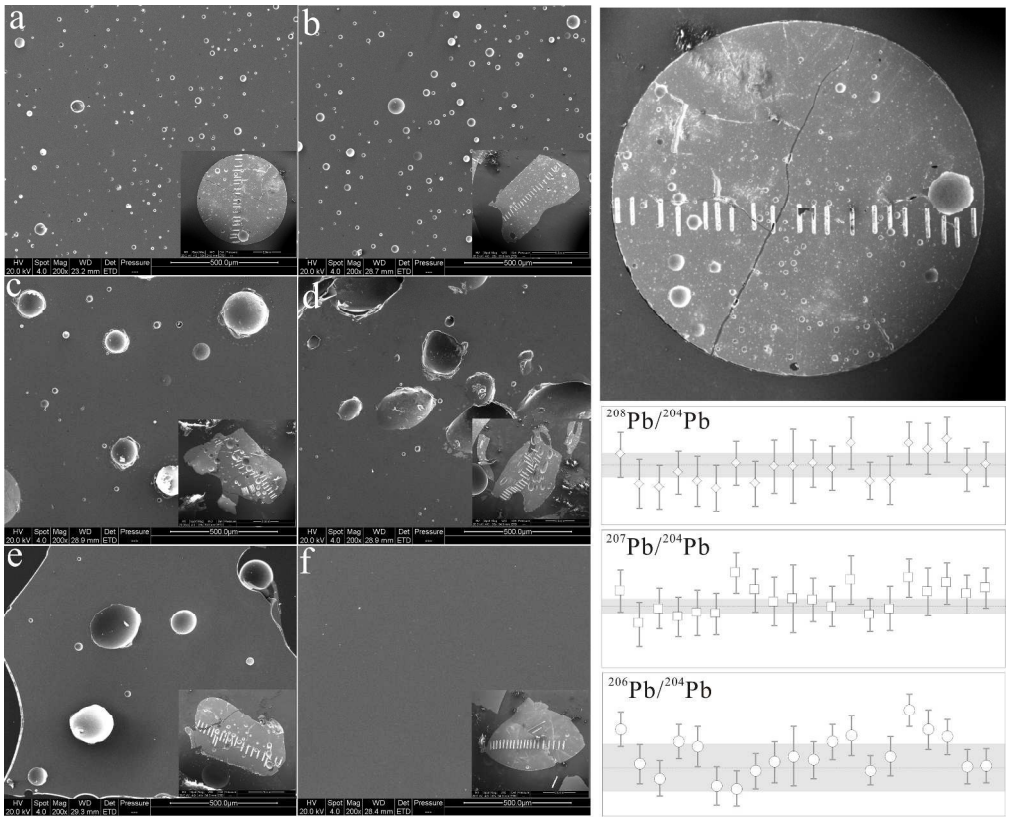

946x767mm (100 x 100 DPI)

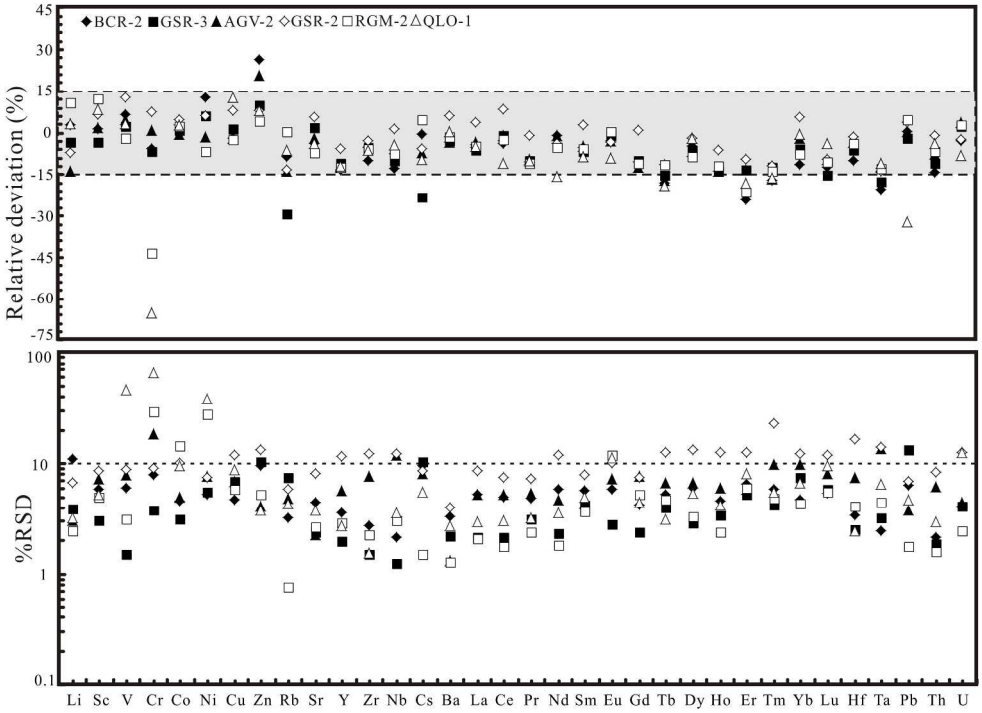

266x192mm (300 x 300 DPI)

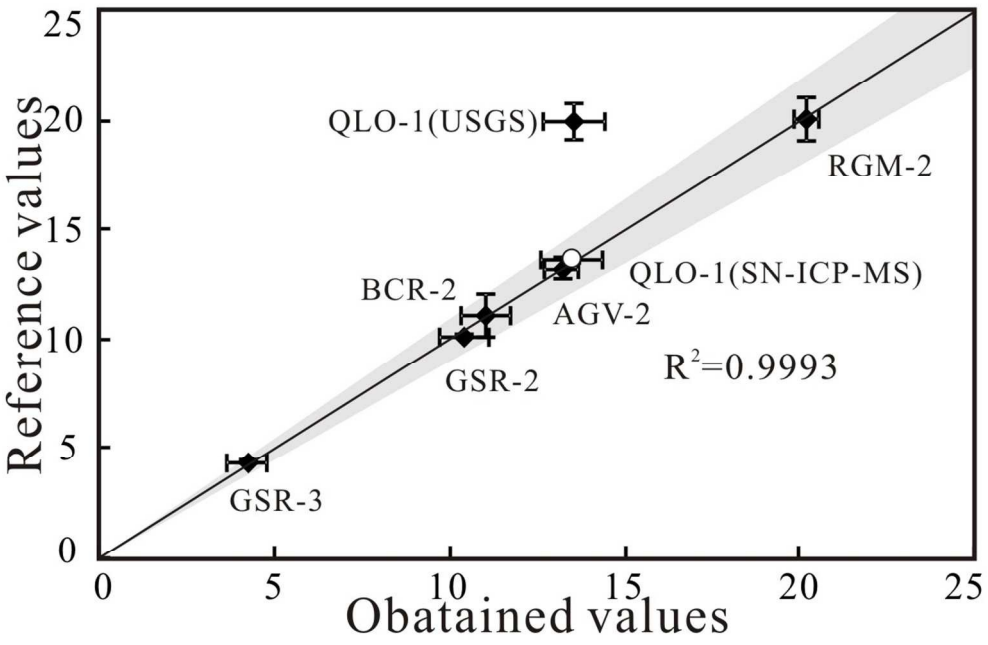

111x72mm (300 x 300 DPI)

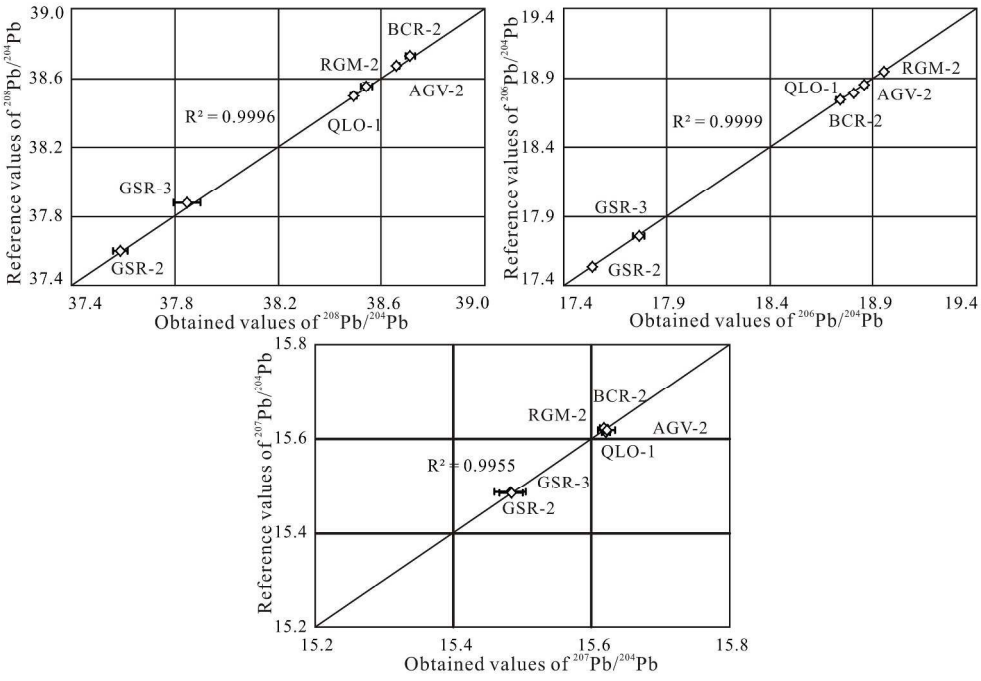

318x219mm (300 x 300 DPI)

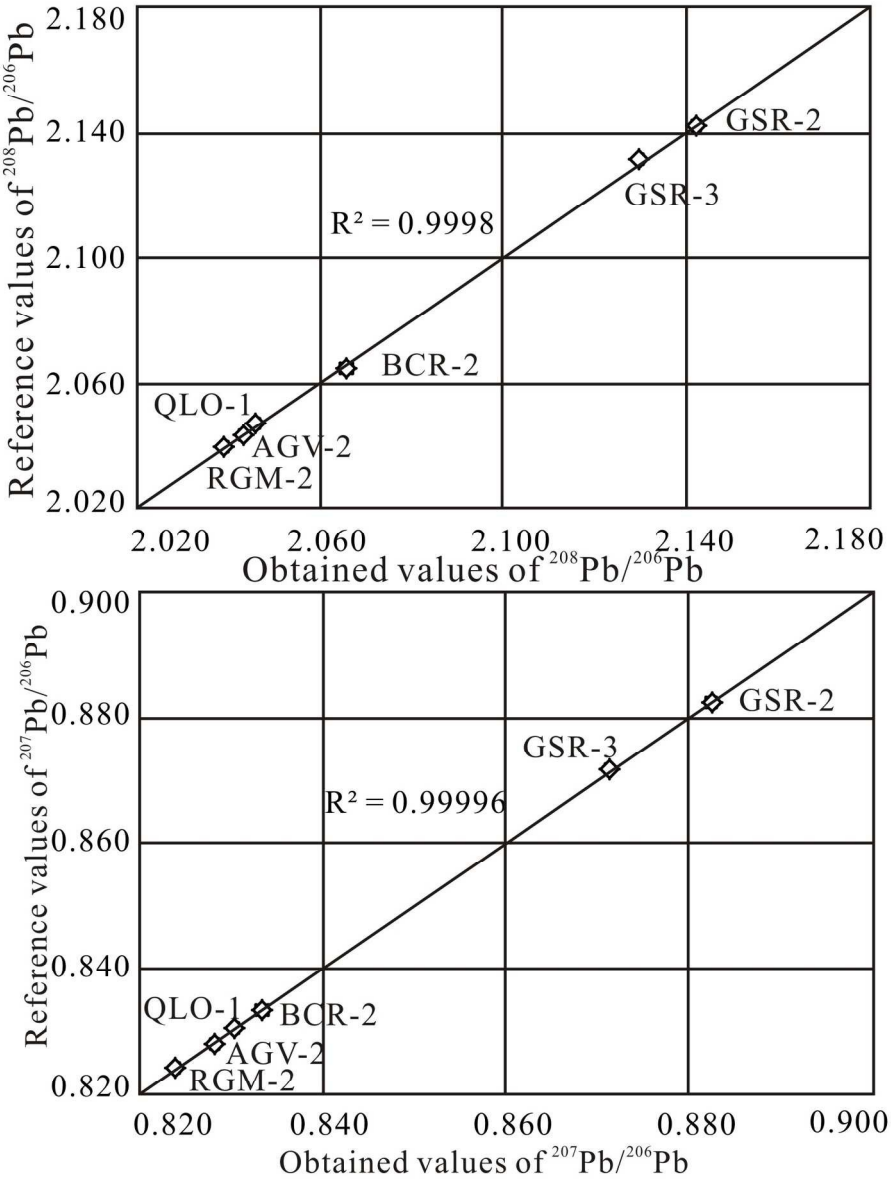

157x210mm (300 x 300 DPI)

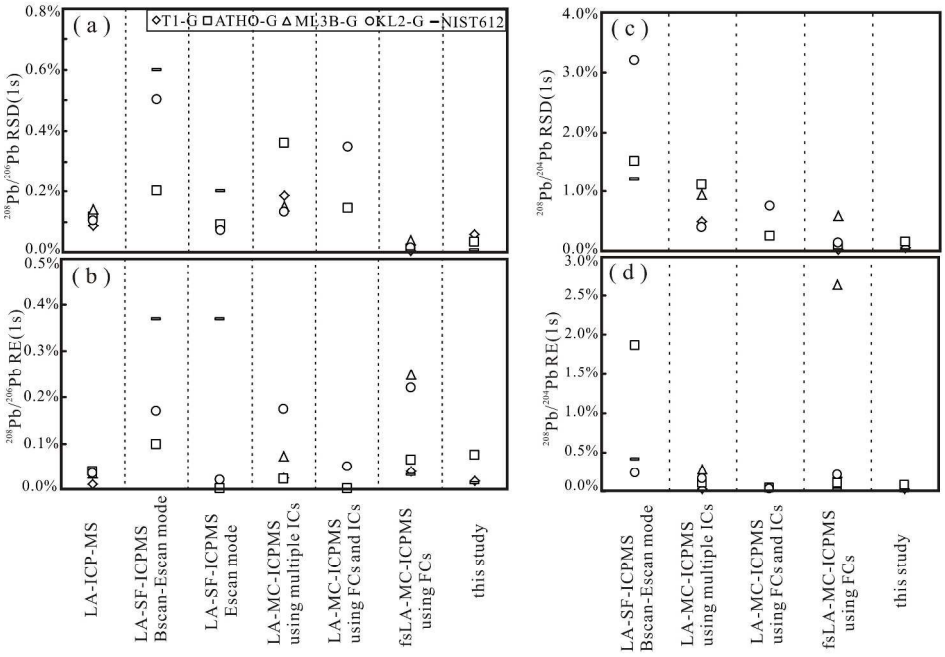

359x244mm (300 x 300 DPI)

Table 1. Operational parameters for ICP-MS and MC-ICP-MS instruments and 193 nm and femtosecond laser ablation systems.

New wave UP Femto 266 nm femtosecond laser system		193 nm laser ablation system (Geolas 2005)	
Laser type	Quantronix Integra-HE	Wavelength	193 nm
Output wavelength	266 nm (ultraviolet)	Energy density	10 J cm^{-2}
Beam profile	>95% fit to Gaussin	Pulse width	15 ns
Beam diameter	1.0 mm	Carrier gas	He, 0.65 L min^{-1}
Pulse duration	<130 fs	Abalation mode	Single spot
Pulse energy output	500 μJ	Abalation spot size	90 μm
Enrgy density	7 J cm^{-2}	Repetition rate	6 Hz
laser beam	65 μm	Background Measuri	20 s
Pulse repetition rate	250 Hz	Signal Measuring Tir	50 s
Carrier gas	He, 0.75 L min^{-1}	Pluses	300
Nu Plasma II MC-ICPMS and Aridus II desolvation nebulizer system		Aglent 7700 ICP-MS	
Plasma gas	13.0 L min^{-1}	RF power	1350 W
Auxiliary gas	0.8 L min^{-1}	Plasma gas	16 L min^{-1}
mix gas	1.0 L min^{-1}	Auxiliary gas	0.8 L min^{-1}
RF power	1300 W	Make-up gas	1.0 L min^{-1}
RF reflected	1 W	Sampler cone	1.0 mm
Accelerating voltage	6000 V	Skimmer cone	0.4 mm
Sensitivity	400 V/ppm Pb isotop	Dwell time	15 ns
Membrane temperatu	160 °C		
Spray chamber tempe	110 °C		
Sweep gas flow	Ar, 3.5 L min^{-1}		

Table 2. Results for the fused RGM-2, QLO-1, AGV-2, GSR-2, BCR-2 and GSR-3 glasses by LA

Element	Isotope	Unit	BCR-2				GSR-3				AGV-2		
			Preferred values		LA-ICP-MS		Preferred values		LA-ICP-MS		Preferred values		LA-IC
			Conc.	1s	Ave.	1s	Conc.	1s	Ave.	1s	Conc.	1s	Ave.
Li	7	μg g^{-1}	9	2	9.2	1.0	10.5	0.1	10.1	0.4	11	1	9.5
Sc	45	μg g^{-1}	33	2	33.4	1.9	15.5	0.1	15.0	0.5	13	1	13.2
V	51	μg g^{-1}	416	14	444	26	174	1	178	3	122	4	125
Cr	53	μg g^{-1}	18	2	17.0	1.3	149	5	139	5	16	1	17.1
Co	59	μg g^{-1}	37	3	38.1	1.7	48.1	0.4	48.5	1.5	16	1	15.9
Ni	60	μg g^{-1}	18	1.00	14.6	0.8	143	1	152	8	20	1	18.7
Cu	63	μg g^{-1}	21	1	18.6	0.9	51.7	0.1	52.4	3.6	53	4	51.9
Zn	66	μg g^{-1}	127	9	160	15	151	1	166	17	86	8	104
Rb	85	μg g^{-1}	46.9	0.1	43.8	1.4	43.1	1.0	30.4	2.2	66.3	2.3	59.2
Sr	88	μg g^{-1}	340	3	332	15	1170	2	1189	28	661	6	644
Y	89	μg g^{-1}	37	2	32	1	24.2	0.1	21.5	0.4	19	2	17.5
Zr	91	μg g^{-1}	184	1	169	5	290	1	275	4	230	4	222
Nb	93	μg g^{-1}	12.6	0.4	11.5	0.2	77.4	0.1	69.4	0.9	14.5	0.8	13.6
Cs	133	μg g^{-1}	1.1	0.1	1.1	0.1	0.46	0.01	0.35	0.04	1.2	0.1	1.08
Ba	137	μg g^{-1}	677	2	660	22	557	1	541	12	1130	11	1099
La	139	μg g^{-1}	24.9	0.2	23.9	1.3	58.2	0.1	54.5	1.1	37.9	0.1	36.7
Ce	140	μg g^{-1}	52.9	0.2	50.9	2.5	106	1	105	2	68.6	0.5	67.1
Pr	141	μg g^{-1}	6.7	0.1	6.1	0.3	12.9	0.1	11.7	0.4	7.84	0.31	7.50
Nd	143	μg g^{-1}	28.7	0.1	27.6	1.6	52.7	0.5	50.0	1.2	30.5	0.1	29.7
Sm	147	μg g^{-1}	6.58	0.02	6.36	0.36	10.7	0.1	9.92	0.41	5.49	0.03	5.41
Eu	151	μg g^{-1}	1.96	0.01	1.94	0.11	3.22	0.01	3.19	0.09	1.53	0.02	1.49
Gd	155	μg g^{-1}	6.75	0.03	6.08	0.26	8.88	0.01	8.00	0.19	4.52	0.05	4.10
Tb	159	μg g^{-1}	1.07	0.03	0.87	0.05	1.11	0.01	0.94	0.04	0.64	0.01	0.53
Dy	163	μg g^{-1}	6.41	0.05	6.09	0.36	5.64	0.03	5.27	0.15	3.47	0.03	3.36
Ho	165	μg g^{-1}	1.28	0.03	1.14	0.05	0.94	0.01	0.81	0.03	0.65	0.03	0.61
Er	166	μg g^{-1}	3.66	0.01	2.77	0.18	1.99	0.01	1.72	0.09	1.81	0.02	1.55
Tm	169	μg g^{-1}	0.54	0.04	0.45	0.03	0.23	0.01	0.20	0.01	0.26	0.01	0.22
Yb	173	μg g^{-1}	3.38	0.02	3.10	0.14	1.27	0.01	1.19	0.09	1.62	0.02	1.56
Lu	175	μg g^{-1}	0.503	0.009	0.445	0.024	0.16	0.01	0.14	0.01	0.247	0.004	0.223
Hf	178	μg g^{-1}	4.9	0.1	4.31	0.15	6.23	0.04	5.83	0.15	5.0	0.1	4.89
Ta	181	μg g^{-1}	0.74	0.02	0.62	0.02	4.39	0.01	3.63	0.11	0.87	0.08	0.78
Pb	208	μg g^{-1}	11	1	11.1	0.7	4.36	0.09	4.27	0.56	13.2	0.5	13.2
Th	232	μg g^{-1}	5.7	0.5	5.30	0.11	6.10	0.01	5.44	0.10	6.1	0.2	5.62
U	238	μg g^{-1}	1.69	0.19	1.64	0.07	1.43	0.01	1.46	0.06	1.86	0.09	1.95

Preferred values of QLO-1, RGM-2, BCR-2 and AGV-2 from GeoReM database; Preferred values of GSR-2 and GSR-3

A-ICP-MS.

	GSR-2				RGM-2				QLO-1			
P-MS	Preferred values		LA-ICP-MS		Preferred values		LA-ICP-MS		Preferred values		LA-ICP-MS	
1s	Conc.	1s	Ave.	1s	Conc.	1s	Ave.	1s	Conc.	1s	Ave.	1s
0.3	20.2	0.1	18.8	1.2	58	3	63.2	1.5	25	2	25.8	0.8
1.0	9.36	0.01	9.94	0.85	5.0	0.3	5.65	0.28	8.9	-	9.63	0.51
10	90.4	0.8	102	9	12.4	1.0	12.2	0.4	54	6	55.7	25.5
3.1	30.2	0.3	32.5	2.9	4.02	0.57	2.26	0.66	3.2	1.7	1.11	0.73
0.8	12.8	0.1	13.4	1.3	2.05	0.10	2.09	0.30	7.2	0.5	7.38	0.70
1.4	18.2	0.2	19.3	1.4	2.38	0.35	2.22	0.60	-	-	2.78	1.05
3.5	55.0	0.6	59.2	6.9	10.5	0.6	10.2	0.6	29	3	32.6	2.9
4	69.2	1.0	74.5	9.8	33.1	1.5	34.4	1.8	61	3	65.8	2.5
2.8	39.6	1.0	34.3	2.0	150	6	151	1	74	3	69.3	2.9
15	809	9	854	69	110	5	102	3	340	12	326	12
1.0	8.99	0.01	8.46	0.98	23.2	1.0	20.3	0.6	24	3	21.2	0.6
17	91.2	2.1	88.6	10.7	228	12	215	5	185	16	174	3
1.6	5.59	0.04	5.67	0.69	9.30	0.47	8.60	0.26	10.0	1.3	9.57	0.34
0.09	1.73	0.01	1.63	0.14	9.86	0.44	10.3	0.2	1.8	0.2	1.63	0.09
14	1021	3	1081	43	848	38	836	11	1370	80	1377	38
1.9	20.9	0.2	21.7	1.9	23.2	0.9	22.1	0.5	27	2	25.7	0.8
3.5	39.1	0.2	42.3	3.2	46.1	1.8	44.9	0.8	54	6	48.1	1.5
0.40	4.66	0.03	4.60	0.33	5.40	0.23	4.79	0.11	6.0	-	5.38	0.17
1.4	19.0	0.1	18.2	2.1	19.5	0.8	18.5	0.3	26	-	21.9	0.8
0.24	3.43	0.03	3.51	0.28	4.09	0.19	3.85	0.14	4.9	0.2	4.46	0.22
0.11	1.09	0.01	1.05	0.11	0.67	0.03	0.67	0.08	1.43	0.12	1.30	0.14
0.31	2.55	0.02	2.57	0.19	3.77	0.18	3.35	0.17	-	-	3.83	0.17
0.04	0.34	0.01	0.30	0.04	0.61	0.03	0.54	0.03	0.71	0.07	0.57	0.02
0.22	1.78	0.01	1.74	0.23	3.78	0.18	3.45	0.11	3.8	0.3	3.73	0.20
0.04	0.31	0.01	0.29	0.04	0.80	0.03	0.71	0.02	-	-	0.74	0.03
0.09	0.84	0.01	0.76	0.10	2.35	0.10	1.85	0.11	2.3	0.1	1.88	0.15
0.02	0.12	0.01	0.10	0.02	0.37	0.02	0.32	0.02	0.37	0.04	0.31	0.02
0.15	0.73	0.01	0.77	0.09	2.57	0.15	2.37	0.10	2.3	0.2	2.29	0.15
0.018	0.11	0.01	0.10	0.01	0.40	0.02	0.36	0.02	0.37	0.40	0.35	0.03
0.36	2.48	0.02	2.44	0.40	5.87	0.27	5.65	0.23	-	-	4.31	0.11
0.10	0.35	0.01	0.30	0.04	0.95	0.04	0.83	0.04	0.82	0.10	0.73	0.05
0.5	10.1	0.1	10.5	0.7	19.3	0.9	20.2	0.4	20.0	0.8	13.5	0.6
0.34	2.63	0.02	2.60	0.21	14.6	0.7	13.6	0.2	4.5	0.5	4.32	0.13
0.09	0.89	0.01	0.87	0.11	5.62	0.25	5.77	0.14	1.90	0.12	1.75	0.22

from Reference 24 and 25; Conc., Concentration; Ave, Average; *s*, standard deviation.

Table 3. Pb isotope ratios for seven reference materials, as measured by SN-MC-ICP-MS.

Sample	$^{208}Pb/^{204}Pb$	$^{207}Pb/^{204}Pb$	$^{206}Pb/^{204}Pb$	$^{208}Pb/^{206}Pb$	$^{207}Pb/^{206}Pb$	Analysis and corection method	Reference
NIST SRM 981	36.7139±12	15.4961±4	16.9399±8	2.16733±8	0.91479±2	MC, Tl, n = 35	10
	36.7219±44	15.4963±16	16.9405±16	2.16771±10	0.91475±2	TS-TIMS, n = 60	32
	36.7225±80	15.4955±26	16.9408±22	2.16770±22	0.91469±6	TIMS	33
	36.7265±20	15.5000±6	16.9418±6	2.16781±8	0.91490±4	DS-MC, n = 26	34
	36.7188±90	15.4942±28	16.9369±34	2.16797±32	0.91481±8	This study, n = 44	
AGV-2	38.544±8	15.619±2	18.862±6	2.04349±74	0.82805±30	This study, n = 18	
	38.552±10	15.621±4	18.873±6			DS-MC, n = 5	34
	38.544±14	15.617±8	18.869±6			MC, n = 7	35
BCR-2	38.721±20	15.624±4	18.750±12	2.06516±90	0.83331±52	This study, n = 14	
	38.723±18	15.624±10	18.757±12			MC, n = 3	36
	38.752±22	15.628±6	18.765±12			DS-MC, n = 8	34
	38.738±18	15.628±2	18.758±10			MC, n = 18	37
	38.724±40	15.625±4	18.753±20			MC, n = 18	35
GSR-3	37.871±8	15.487±4	17.768±2	2.13144±30	0.87165±10	this study,N=8	
GSR-2	37.594±10	15.486±2	17.545±8	2.14272±56	0.88262±30	this study,N=8	
QLO-1A	38.484±6	15.614±2	18.797±2	2.04734±30	0.83065±8	this study,N=8	
RGM-2	38.660±8	15.618±2	18.950±10	2.04010±72	0.82414±46	this study,N=8	

All values presented as mean ± 2*s*. SN-MC-ICP-MS, solution-nebulizer multicollector inductively coupled plasma mass spectrometry; NIST, National Institute of Standards and Technology; DS, double-spike; TIMS, thermal ionization mass spectrometry.

Table 4.Pb isotope ratios measured in fused glasses of six reference materials,NIST SRM 610 and NIST SRM 612 by fsLA-MC-ICP-MS and confirmed by SN-MC-ICP-MC.

Sample		$^{208}Pb/^{204}Pb$	$^{207}Pb/^{204}Pb$	$^{206}Pb/^{204}Pb$	$^{208}Pb/^{206}Pb$	$^{207}Pb/^{206}Pb$
NIST SRM 610	Chen et al.[10]	36.980±7	15.515±3	17.052±3	2.1686±1	0.90985±5
	Jochum et al.[17]	36.964±22	15.504±9	17.045±8	2.1680±10	0.9096±3
	Shaheen and Fryer[38]	36.972±14	15.509±5	17.047±5	2.1685±3	0.9097±1
	fsLA-MC-ICP-MS	36.972±8	15.512±3	17.052±4	2.1681±3	0.90973±16
	1RSD (%)	0.011	0.01	0.011	0.008	0.009
	1RSE (%)	0.006	0.005	0.005	0.002	0.001
NIST SRM 612	Chen et al.[10]	36.995±9	15.513±4	17.096±4	2.1640±1	0.90740±4
	Jochum et al.[17]	37.005±10	15.511±3	17.095±2	2.1647±4	0.90730±10
	fsLA-MC-ICP-MS	37.005±12	15.514±6	17.094±6	2.1650±4	0.90761±20
	1RSD (%)	0.015	0.016	0.018	0.009	0.011
	1RSE (%)	0.047	0.047	0.047	0.006	0.005
RGM-2	fsLA-MC-ICP-MS	38.659±20	15.620±8	18.955±17	2.0392±12	0.82398±66
	SN-MC-ICP-MS	38.660±8	15.618±2	18.950±10	2.0401±8	0.82414±46
	1RSD (%)	0.026	0.027	0.045	0.029	0.040
	1RSE (%)	0.041	0.041	0.041	0.005	0.006
	RE (%)	-0.004	0.013	0.029	-0.046	-0.019
QLO-1	fsLA-MC-ICP-MS	38.491±26	15.621±12	18.809±17	2.0463±13	0.83042±63
	SN-MC-ICP-MS	38.484±14	15.614±4	18.797±4	2.0473±6	0.83065±14
	1RSD (%)	0.034	0.037	0.045	0.032	0.038
	1RSE (%)	0.065	0.065	0.066	0.006	0.007
	RE (%)	0.019	0.046	0.064	-0.051	-0.028
AGV-2	fsLA-MC-ICP-MS	38.542±45	15.622±26	18.860±23	2.0433±13	0.82824±84
	SN-MC-ICP-MS	38.544±16	15.619±4	18.862±14	2.0435±14	0.82805±62
	1RSD (%)	0.059	0.082	0.062	0.032	0.051
	1RSE (%)	0.122	0.122	0.123	0.009	0.011
	RE (%)	-0.006	0.018	-0.012	-0.011	0.023
GSR-2	fsLA-MC-ICP-MS	37.588±55	15.483±34	17.544±25	2.1424±16	0.88240±83
	SN-MC-ICP-MS	37.594±18	15.486±4	17.545±14	2.1427±12	0.88262±60
	RSD (%)	0.073	0.109	0.070	0.037	0.047
	RSE (%)	0.121	0.121	0.121	0.013	0.017
	RE (%)	-0.016	-0.017	-0.007	-0.014	-0.024
BCR-2	fsLA-MC-ICP-MS	38.711±37	15.618±13	18.740±35	2.0656±24	0.83338±118
	SN-MC-ICP-MS	38.721±20	15.624±4	18.750±14	2.0652±10	0.83331±52
	1RSD (%)	0.047	0.041	0.092	0.057	0.071
	1RSE (%)	0.096	0.096	0.097	0.007	0.010
	RE (%)	-0.025	-0.039	-0.055	0.018	0.008
GSR-3	fsLA-MC-ICP-MS	37.847±107	15.482±46	17.767±54	2.1298±13	0.87131±68
	SN-MC-ICP-MS	37.871±18	15.487±6	17.768±4	2.1314±6	0.87165±20
	1RSD (%)	0.142	0.147	0.153	0.032	0.039
	1RSE (%)	0.191	0.191	0.191	0.012	0.015
	RE (%)	-0.064	-0.034	-0.004	-0.073	-0.039

All values presented as mean ± 2s. MC-ICP-MC: multicollector inductively coupled plasma mass spectrometry; fsLA, femtosecond laser ablation; SN, solution nebulizer; RSD, relative standard deviation; RSE, relative standard error; RE, relative error.